

# Experimental and numerical investigation of the effect of off-fault damage on dynamic earthquake rupture propagation

*H. S. Bhat*<sup>1,2</sup>, R. L. Biegel<sup>1</sup>, A. J. Rosakis<sup>2</sup>, C. G. Sammis<sup>1</sup>

1. *University of Southern California, Los Angeles, USA;*

2. *California Institute of Technology, Pasadena, USA;*

E-mail: *hbhat@usc.edu*

## 1 Abstract

Real earthquake faults are surrounded by fractured zones whose effect on earthquake rupture is investigated. We first performed a series of dynamic photoelasticity experiments of a dynamic shear rupture along a frictional interface bounded on one side by an intact material and on the other side by a damaged material of the same or different undamaged elastic properties. We notice that on the side of the rupture where damage is in tension the bulk damage effects dominate over the local elastic effects leading to reduction in rupture velocity or in some cases complete termination while on the compressional side the local elastic effect seems to dominate. To numerically model the above experiments we developed a micro-mechanics based damage constitutive description with friction on the fault governed by complex rate and state like laws. Our numerical results agree well with the photoelastic experiments.

## 2 Introduction

Although earthquakes are commonly modeled as frictional instabilities on planar faults, real faults, many of which have been exhumed from seismogenic depths, have a more complex structure shown schematically in Figure 1. Most slip occurs in a highly sheared “core”, typically a few centimeters thick, and composed of extremely fine grained granulated rock (known as cataclasite) which is commonly altered to clay mineralogy, particularly as shallow depths. Slip within the core is often localized onto principal slip surfaces a few mm thick and composed of still finer grained

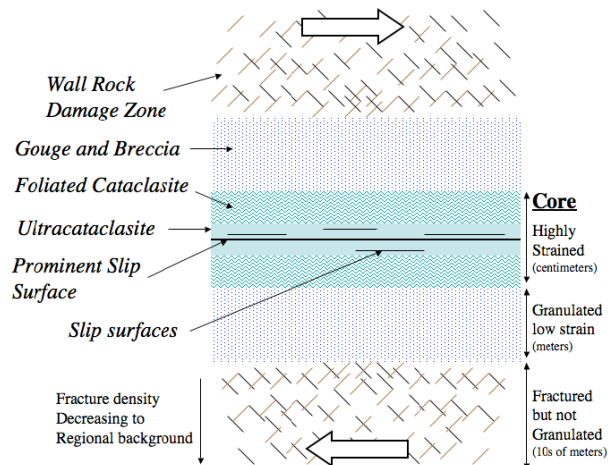


**Figure 1: Schematic cross-section of an idealized fault at seismogenic depth. The nested layered structure is described in the text. The widths of the layers vary from fault to fault, and the structure is often less symmetric than shown here.**

mm thick and composed of still finer grained

ultracataclasites. The core is bordered by layers of coarser granulated rock commonly termed gouge or fault breccia, or more recently pulverized rock. These layers are typically meters thick and appear to have accommodated little or no shear strain. The granular layers are bordered by highly fractured (but not granulated) wall rock within which the fracture density decreases to the regional background value over a distance of a few hundred meters. More detailed descriptions of fault zone structure, deviations from the ideal symmetry in Figure 1, and discussions as to how it might have formed are given by [1, 2].

The focus of this paper is on how fault zone structure affects earthquake rupture propagation, with special emphasis on a series of recent laboratory measurements of rupture velocity on faults in damaged photoelastic plates by [3, 4] and [5]. [3] observed a reduction in rupture velocity caused by a symmetric distribution of damage about a pre-machined fault and measured the spatial extent of the interaction between the rupture tip and the off-fault damage. [4] and [5] studied propagation asymmetries caused by slip on the interface between damaged and undamaged materials, as would be the case if an earthquake rupture propagated along one side of a fault zone.

A first order effect of fracture damage on rupture propagation is to lower the elastic stiffness of the material. By reducing the shear wave speed  $c_s$ , the effect on rupture velocity is to lower the limiting Rayleigh speed, which is  $0.92c_s$  for Mode II ruptures. However, [3] found that damage reduced the rupture velocity below that expected based solely on the lower shear wave speed. They ascribed this additional reduction to a further dynamic reduction in modulus and to anelastic losses associated with frictional slip on the myriad of small off-fault fractures that comprise the damage. [4] and [5] extended these measurements to ruptures that propagate on the interface between damaged and undamaged materials. In these experiments, the off-fault damage produced additional asymmetries in the propagation of ruptures beyond those expected from the associated contrast in elastic stiffness. Propagation asymmetries ascribed to the damage were observed to be stronger than those due to elastic contrasts.

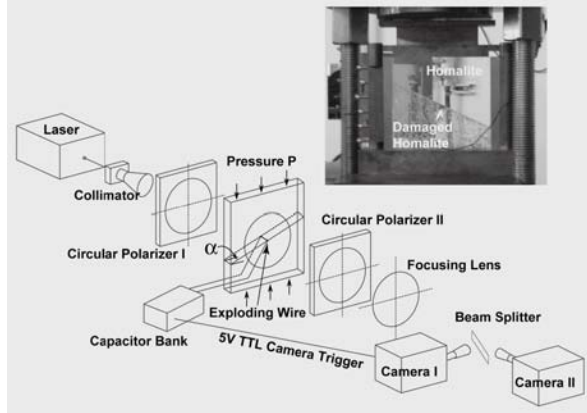


**Figure 2: Schematic diagram of apparatus used to take a series of high-speed photographs of dynamic ruptures on pre-machined faults in photoelastic Homalite and polycarbonate plates. The inset shows a sample in the loading frame used to apply uniaxial stress  $P$ .**

### 3 Experimental Apparatus

All experiments described here used the apparatus shown in Figure 2. Square plates of the photoelastic polymers Homalite and polycarbonate were prepared with a pre-machined fault at an angle  $\alpha$  to the edge as in Figure 3. The plates were loaded with a uniaxial stress  $P$  and a bilateral rupture was nucleated by using a high-voltage pulse to explode a wire in a small hole that crossed the center of the fault plane. The explosion reduced the normal stress on an  $\sim 1$  cm long patch of the fault plane allowing shear slip that nucleated the rupture. The voltage pulse was also used to trigger a pair of high-speed digital cameras that recorded a series of high-speed images of the shear stress field revealed as fringes in polarized laser light.

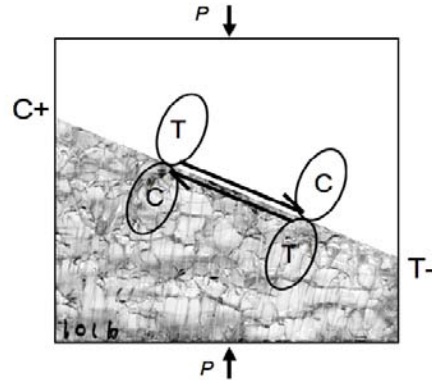


**Figure 3: Asymmetries in an undamaged Homalite plate in contact with a damaged Homalite plate. Since the damaged Homalite is slightly less stiff than the undamaged Homalite, the ‘+’ direction of propagation is to the left, which by convention is the direction of motion of the less stiff material. The anelastic asymmetry is denoted by the ‘C’ propagation direction for which the compressional lobe of the crack tip stress concentration travels through the damage and the ‘T’ direction for which the crack tip places the damage in tension.**

The upper panel in Figure 4 shows four frames taken at the times indicated during one of the Homalite experiments. Fringes associated with stress concentration at the rupture fronts and S wave (generated by the nucleation event) can be identified. The lower panel in Figure 4 shows the corresponding instantaneous velocity as a function of time. Instantaneous velocity was found by differentiating an interpolated cubic spline fit to the displacements using a MATLAB utility [4, 5]. Note that propagation is symmetric and both rupture tips accelerate to the limiting (Rayleigh) rupture velocity for mode II propagation and then transition to supershear velocities approaching the P wave speed (note,  $c_p/c_s = 2.1$  for Homalite).

### 4 Effect of Asymmetric Off-Fault Damage on Rupture Velocity and Directionality

[4] used the apparatus in Figure 2 to measured the velocity of ruptures on the interface between damaged and undamaged Homalite. As illustrated in Figure

3, the symmetry in these experiments is broken in two ways: elastically and anelastically. The elastic asymmetry is caused by the change in elastic modulus across the fault plane, and results in different propagation velocities in the ‘+’ direction (the direction in which the lower velocity damaged Homalite moves) and in the opposite ‘-’ direction. The physical cause of this elastic asymmetry is tension across the fault plane at the tip of the rupture propagating in the ‘+’ direction [6, 7, 8, 9, 10, 11, 12, 13, 14].

Prior experimental studies in such elastic bi-materials by [12] found that ruptures in the ‘+’ direction propagate at the generalized Rayleigh wave speed while those in the opposite ‘-’ direction transition to super shear velocities that approach  $P_{slow} \equiv c_P^{slow}$ , the P wave speed in the material having slower wave speeds. Theoretical studies have shown that, depending on the friction law and loading conditions, a transition to supershear propagation is also possible in the ‘+’ direction with velocity approaching  $P_{fast} \equiv c_P^{fast}$ , the P wave speed in the material having faster wave speeds [8, 10]. [5] observed simultaneous supershear propagation in the ‘+’ direction at  $P_{fast}$  and in the ‘-’ direction at  $P_{slow}$ .

We hypothesize that the anelastic asymmetry arises because one fracture tip has the compressive lobe of its stress concentration in the damage (which we term the ‘C’ direction) while the other tip has its tensile lobe in the damage (which we term the ‘T’ direction). For example, in Figure 4 the rupture tip moving to the

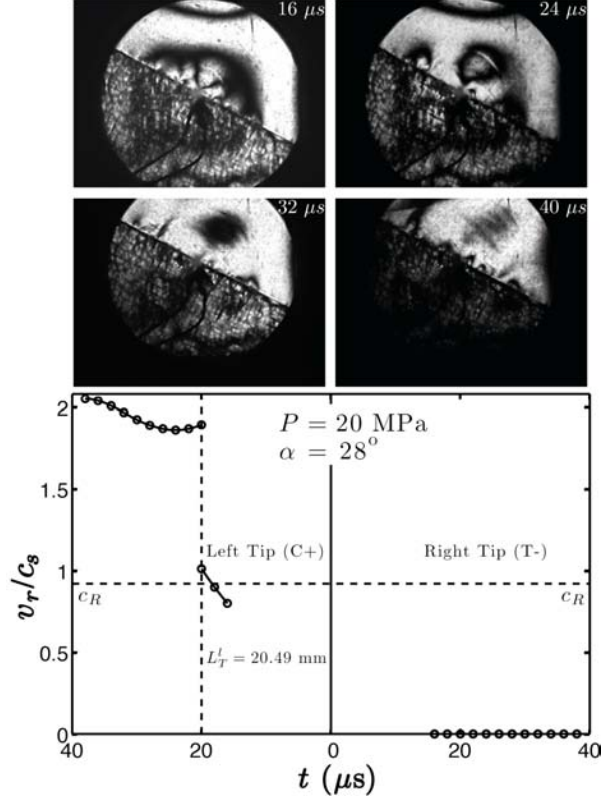


**Figure 4: Dynamic rupture on the interface between damaged and undamaged Homalite plates. The upper four panels show frames at the times indicated selected from the sequence of high-speed photographs. The lower panel shows the instantaneous velocity of the rupture tips as a function of time. Note that the left tip propagating in the ‘C+’ direction transitions to supershear but that rupture propagation in the ‘T-’ direction is completely suppressed, presumably by energy loss on the off fault damage activated by the tensile lobe of the stress field.**

left is labeled ‘C+’ because it is moving in the ‘+’ direction ( the direction of motion of the more compliant damaged Homalite) and ‘C’ because the compressive stress concentration lies in the damage. Following this convention, the tip moving to the right is labeled ‘T-’. We propose that the physical cause of the anelastic asymmetry is that tension in the ‘T’ direction enhances sliding on the off-fault cracks that comprise the damage while compression in the ‘C’ direction suppresses sliding. This asymmetry is evident in Figure 5 which shows the velocities measured by [4] for a rupture on the interface between damaged and undamaged Homalite. Note that the rupture running in the ‘C+’ direction moves at  $P_{fast}$ , the expected velocity in

the ‘+’ direction for an elastic bi-material. Off-fault damage appears to have little additional effect in the ‘C’, presumably because sliding is suppressed by the crack-tip compression. However, note that the rupture in the ‘T-direction stops. The interpretation is that tension enables energy dissipation by frictional sliding in the off-fault damage near the crack tip that completely suppresses propagation.. The full set of rupture velocities measured by [4] on interfaces between Homalite and damaged Homalite are summarized in Figure 5 where they are compared with measurements at the same loads for the undamaged Homalite system.

Note that ruptures in the ‘C+’ direction are only slightly affected by the damage while those in the ‘T-’ direction are severely slowed or even stopped, especially at the highest loads. The rupture velocity in the all-damaged Homalite is seen to be the same as the velocity in the ‘T-’ direction on the interface between Homalite and damaged Homalite (also at 12 MPa). This is the expected result based on our hypothesis that the compressional side of the rupture doesn't see the damage.

[5] extended this work by measuring rupture velocities on the interface between damaged Homalite and undamaged polycarbonate (which has a slightly lower shear wave speed than does damaged Homalite). However, for comparison, they first measured the velocity of ruptures on the interface between

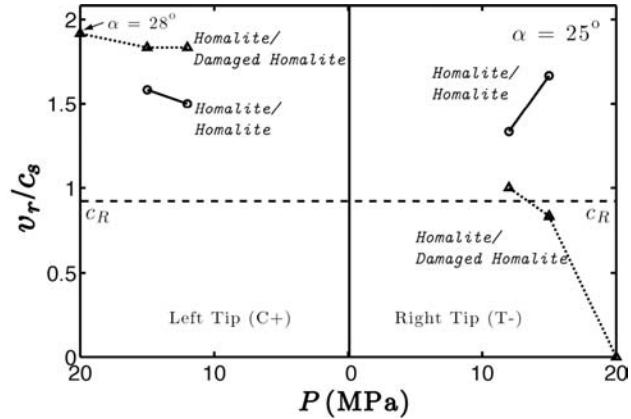


**Figure 5: Summary of experimental results comparing rupture velocity in damaged bimaterial samples with those in undamaged Homalite plates. Note that the off-fault damage has little effect on ruptures traveling in the ‘C+’ direction but a large effect on those propagating in the ‘T-’ direction. Bimaterial ruptures having the tensile lobe in the damage did not transition to supershear and, at large uniaxial loads, did not propagate at all [from 4].**

undamaged Homalite and undamaged polycarbonate. The results of a typical experiment are shown in Figure 6 where four frames of the high-speed sequence (taken at the times indicated) are shown in the upper panel and the velocities are shown in the lower panel. Note that left rupture propagating in the ‘+’ direction transitions to supershear velocities approaching  $P_{fast}$  while the right rupture propagating in the ‘-’ direction approaches  $P_{slow}$ . This bimaterial system was explored in more detail by [12], although they never observed supershear in both directions probably because the propagation distance to the supershear transition in their experiments was longer than the radius of the observable circle due to their rougher sliding surfaces (see [15] for a discussion of the supershear transition length).

Since undamaged polycarbonate has a lower elastic stiffness than does damaged Homalite, propagation directions in these experiments are ‘T+’ to the left and ‘C-’ to the right. Note that in the T-direction the rupture velocity approaches the generalized Rayleigh speed while in the C+ direction it slowly increases toward  $P_{slow}$ , the P wave speed in polycarbonate. The full set of rupture velocities measured by [5] on interfaces between damaged Homalite and polycarbonate are summarized in Figure 7 where they are compared with the measured velocity of ruptures at the same loads on the interface between undamaged Homalite and polycarbonate. As in the previous case of Homalite in contact with damaged Homalite, ruptures in the ‘C’

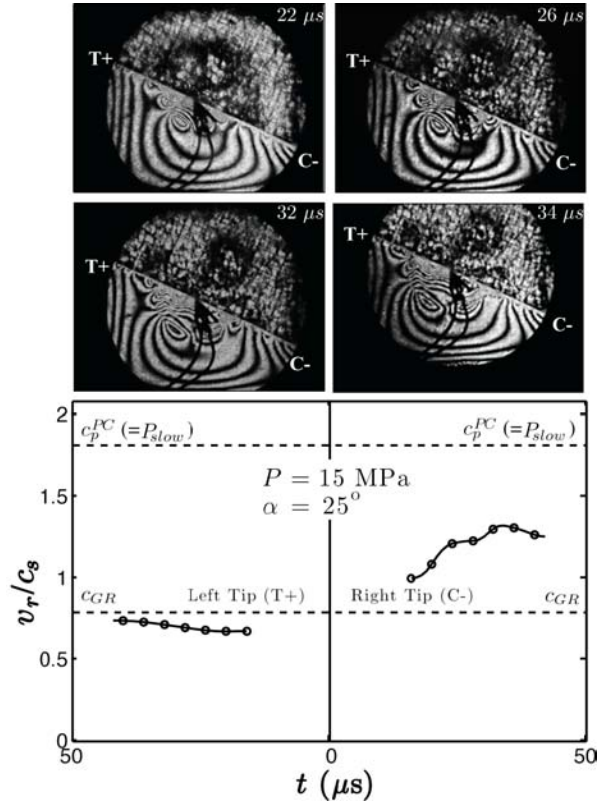


**Figure 6:** Dynamic rupture on the interface between damaged Homalite and undamaged polycarbonate plates. The upper four panels show frames at the times indicated selected from the sequence of high-speed photographs. The lower panel shows the instantaneous velocity of the rupture tips as a function of time. Note that the left tip propagating in the ‘C-’ direction transitions to supershear but that rupture propagation in the ‘T+’ direction does not transition to supershear, presumably due to energy loss on the off-fault damage activated by the tensile lobe of the stress field [from 5].

direction are only slightly affected by the damage. Like rupture velocities in the undamaged system, they appear to be increasing toward  $P_{slow}$ , but only at higher loads. Ruptures in the ‘T’ direction are more severely affected by the damage. The transition to supershear, which takes place in the undamaged system, is suppressed in the damaged system where ruptures propagated at the generalized Rayleigh speed for applied loads up to 15 MPa.

## 5 Modeling Off-fault Damage During Dynamic Rupture Propagation

In order to include the effects of off-fault damage in a numerical dynamic rupture mode in a physically sound way, there are three requirements. The model

should allow for accumulation of permanent deformation. This seems logical as one can imagine the micro-cracks surrounding a fault core accommodating some anelastic slip as the transient stress field from the main rupture passes through them. The presence of micro-cracks should affect the elastic moduli of solids. The change in the elastic moduli will depend on the amount of slip or opening on the micro-cracks which in turn depends on the state of stress in the medium. The model should thus allow for dynamic change in elastic modulus with changing stress and strain. The model also requires a physical criterion for creation of fresh micro-cracks and/or extension of pre-existing ones.

The key to modeling the interaction between off-fault damage and a dynamic rupture lies in properly accounting for energy dissipation in the medium, and this requires a physical model for the micro-cracks in the constitutive description. Extensive work in this area is available in the engineering literature [e.g. 16, 17, 18, 19, 20] but the constitutive descriptions are problem-specific since approximations are required if the model is to be computationally tractable. For dynamic earthquake problems the constitutive model can ignore large strains and rotations in the medium but cannot ignore the generation and extension of fracture damage. Also proper modeling of frictional dissipation on

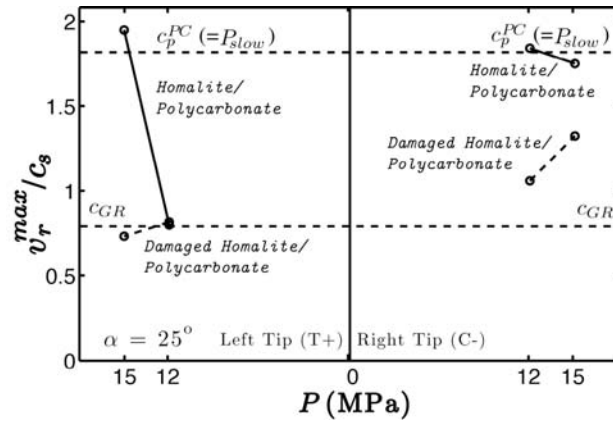


**Figure 7: Summary of experimental results comparing rupture velocity in damaged and undamaged bimaterial plates. Note that the off-fault damage has little effect on ruptures traveling in the C- direction but a large effect on those propagating in the T+ direction. Bimaterial ruptures having the tensile lobe in the damage did not transition to supershear [from 5].**

the micro-cracks will be required as lab studies by [3, 4] have found this to be an important source of off-fault energy dissipation.

The earliest attempt to address off-fault energy dissipation was [21] who, using the self-consistent scheme of [22], derived macroscopic stress strain relations for an elastic solid with non-interacting cracks (straight in 2D or circular in 3D) oriented perpendicular to either maximum tension axis or maximum compression axis. In addition to the modified Lam elastic constants an additional parameter, directly related to crack density, was introduced that accounted for non-linear behavior at even small strains (less than 0.1%). [23] subsequently introduced kinematic aspects of the damage rheology by introducing a scalar damage state variable based on thermodynamic arguments. The evolution of this damage state variable depends on the elastic strain energy density. A key feature of this model is the incorporation of logarithmic healing making it a good candidate for modeling fault structure evolution over a large number of seismic cycles.

More recently, [24], building upon [25], developed a damage mechanics model that is ideal for dynamic rupture propagation problems. [25] studied the onset of failure in damaged rocks by evaluating the state of stress in rock where damage was modeled as a distribution of interacting cracks (straight in 2D or circular in 3D) having tensile wing cracks emanating from their ends. [24] expanded this model for more general states of stress, assuming that the third stress invariant,  $J_3$ , is zero, and added a time dependent law for the growth of the wing cracks. Their model explicitly addresses three stress regimes under which a damaged elastic solid may operate:

*Regime I:* In this regime the initial cracks are shut and stresses on them are below the Coulomb slip criterion. Hence they have no influence on the elastic moduli of the solid and the elastic strain energy density is given by

$$W = W_0 = \frac{1}{4G} \left[ \frac{2}{3}\sigma_e^2 + \frac{3(1-2\nu)}{1+\nu}\sigma_m^2 \right] \quad (1)$$

where  $\nu$  is the Poisson ratio of the undamaged elastic solid,  $\sigma_e = \sqrt{3}/2(\sigma_3 - \sigma_1)$ ,  $\sigma_m = (\sigma_1 + \sigma_3)/2$  and  $\sigma_3 \geq \sigma_2 \geq \sigma_1$  are the principal stresses.

*Regime II:* Sliding on the initial flaws leads to tension on the wing cracks. The elastic strain energy density is given by (assuming that the length of the wing crack  $l$  is small compared to the main crack size  $a$ )

$$W = W_0 + \frac{\pi D_0}{4\alpha^3 G(1+\nu)} [A\sigma_m + B\sigma_e]^2 \quad (2)$$

where  $G$  is the shear modulus of the undamaged solid and  $\alpha = \cos \Psi$ . Only the most damaging cracks are considered and hence  $\Psi = 45^\circ$ .  $A$  and  $B$  depend on the geometry of the crack, the co-efficient of friction needed to overcome

sliding, and a non-dimensional measure of damage,  $D/D_0$ .  $D_0$  is the initial damage in the material and  $D$  is the current damage; they are defined as:

$$D_0 = \frac{4}{3}\pi(\alpha a)^3 f ; D = \frac{4}{3}\pi(l + \alpha a)^3 f \quad (3)$$

where  $f$  is the crack density defined as number of cracks per unit volume. In its current form the model does not account for frictional dissipation but this is easily rectified if the co-efficient of friction is treated as a state variable along with damage parameter  $D$  and is allowed to evolve with slip or slip rate. We are in the process of incorporating that mechanism into the model. The wing cracks are allowed to grow according to a growth law that is modeled on stress corrosion mechanism. Thus

$$\dot{l} = \min \left[ \dot{l}_0 (K_I/K_{IC})^m, c_s \right] ; 10 \leq m \leq 20 \quad (4)$$

where  $K_{IC}$  is the critical stress intensity factor for Mode-I fractures (for rocks  $K_{IC} = 1\text{MPa}\cdot\text{m}^{1/2}$ ),  $K_I$  is the Mode-I stress intensity factor at the tip of the wing crack and  $c_s$  is the shear wave speed of the medium. Since  $D$  depends on  $l$  we have a mechanism for damage evolution that sees damage evolution as the growth of wing cracks.

*Regime III:* In this regime there is loss of contact on the initial cracks and the damaged elastic solid is modeled as a Budiansky-OConnell solid as in [21]. In this case

$$W = W_0 + \frac{\pi D_0}{4\alpha^3 G(1 + \nu)} \left[ C^2 \sigma_m^2 + D^2 \sigma_e^2 \right] \quad (5)$$

where  $C$  and  $E$  are related to  $A$  and  $B$  above by ensuring continuity of elastic strains as one transitions between regimes *II* and *III*. Thus

$$C = A + \gamma \sqrt{\alpha \left( \frac{D}{D_0} \right)^{1/3}} ; E^2 = \frac{B^2 C^2}{C^2 - A^2} \quad (6)$$

where  $\gamma = 2.0$  is a crack shape factor. The corresponding elastic strains are then obtained from  $W$  as

$$\epsilon_{ij} = \frac{\partial W}{\partial \sigma_{ij}} \quad (7)$$

The model is now complete except for parameterizing the transition between regimes. To that end define triaxiality,  $\lambda = \sigma_m/\sigma_e$ . In regime *I*,  $\lambda \leq -B/A$ . Transition from regime *II* to *III* occurs when  $\lambda = AB/(C^2 - A^2)$ .

## 6 Results

We used the above constitutive description to simulate rupture on a planar interface between intact elastic solid and damaged elastic solid. The calculations were done under 2D plane strain conditions for rock-like materials. The material properties used are described in Figure 8. Rupture was nucleated at

the interface by dropping the static and dynamic co-efficient of friction along a finite part of the interface whose length was 10% greater than a critical crack length required for the onset of dynamic rupture instability.

Broadly speaking, the results are in agreement with the experimental observations. However, several key issues need to be addressed. Firstly, the interface is locally bounding bi-material solids and hence the question of ill-posedness (Ranjith and Rice, 2001) needs to be explored. Secondly, the damage mechanics does not yet have any frictional dissipation. We suspect that the damage effects will be even

more dramatic under such circumstances. Thirdly, the role of various friction laws in dynamic rupture propagation has yet to be investigated. The slip-weakening friction used in this simulation can produce only crack-like ruptures. The dynamics of the interaction between

a rupture and the damaged elastic solid should change dramatically when a pulse-like rupture propagates along the interface.

## 7 Discussion

An asymmetric distribution of off-fault damage in a fault zone has been shown to produce strongly directional propagation on the fault plane. The physical source of this directionality is hypothesized to be the interaction between the crack-tip stress field and the off-fault fractures. Ruptures travel more slowly in the ‘T’ direction for which the tensile lobe of the stress concentration travels through the damage. By comparison, ruptures that travel in the ‘C’ direction for which the compressive lobe in the damage propagate as if there were no off-fault damage. Our physical interpretation is that crack-tip compression immobilizes off-fault cracks while crack tip tension enhances frictional slip. It is surprising that the directionality observed in laboratory experiments is so strong (see summaries in Figures 5 and 7), especially since there was no evidence that new damage was created. Stress concentrations at the rupture front of real earthquakes were estimated by [26] to be capable of generating new damage to distances of meters from the fault plane. The generation of new damage is expected to make directional propagation even stronger.

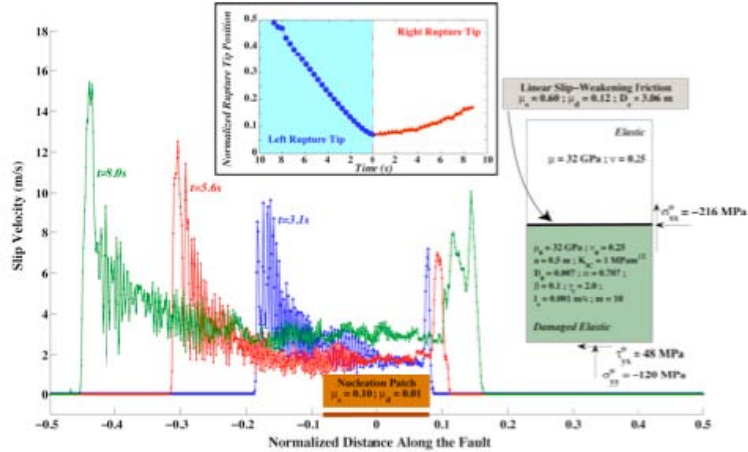


**Figure 8: Snap shots of slip velocity along the interface between intact and damaged elastic solids. Inset: Position of the left and right rupture tips as a function of time.**

The [26] dynamic slip pulse model provides guidance as to how the interaction between the rupture front and off-fault damage scales from the laboratory experiments discussed here and real earthquakes. The spatial extent of the interaction is quantitatively related to the ratio of the rupture velocity to the shear wave speed, the orientation of the remote “tectonic” stress field relative to the fault plane, the dynamic stress drop, and the slip weakening distance (or, equivalently, the fracture energy). These scaling relations have been validated, to first order, by the experiments in photoelastic plates discussed here.

## 8 Acknowledgements

The authors acknowledge support of the National Science Foundation collaborative grant EAR-0711171 to the University of Southern California and the California Institute of Technology. This research was supported by the Southern California Earthquake Center. SCEC is funded by NSF Cooperative Agreement EAR-0106924 and USGS Cooperative Agreement 02HQAG0008.

## 9 References

- [1] Y. Ben-Zion and C. G. Sammis. Characterization of Fault Zones. *Pure Appl. Geophys.*, 160(3):677–715, 2003.
- [2] R. L. Biegel and C. G. Sammis. Relating fault mechanics to fault zone structure. *Adv. Geophys.*, 47:65–111, 2004.
- [3] R. L. Biegel, C. G. Sammis, and A. J. Rosakis. An experimental study of the effect of off-fault damage on the velocity of a slip pulse. *J. Geophys. Res.*, 113(B4), 2008.
- [4] R. L. Biegel, H. S. Bhat, C. G. Sammis, and A. J. Rosakis. The Effect of Asymmetric Damage on Dynamic Shear Rupture Propagation I: No Mismatch in Bulk Elasticity. *J. Geophys. Res. (subm.)*, 2008.
- [5] H. S. Bhat, R. L. Biegel, A. J. Rosakis, and C. G. Sammis. The Effect of Asymmetric Damage on Dynamic Shear Rupture Propagation I: With Mismatch in Bulk Elasticity. *J. Geophys. Res. (subm.)*, 2008.
- [6] J. Weertman. Unstable slippage across a fault that separates elastic media of different elastic constants. *J. Geophys. Res.*, 85(83):1455–1461, 1980.
- [7] R. A. Harris and S. M. Day. Effects of a low-velocity zone on a dynamic rupture. *B. Seismol. Soc. Am.*, 87(5):1267–1280, 1997.
- [8] A. Cochard and J. R. Rice. Fault rupture between dissimilar materials—Ill-posedness, regularization, and slip-pulse response. *J. Geophys. Res.*, 105(B11), 2000.
- [9] J. R. Rice. New perspectives on crack and fault dynamics. *Mechanics for a New Millennium*, pages eds. H. Aref and J. W. Phillips, Kluwer Academic Publishers, 1–23, 2001.
- [10] K. Ranjith and J. R. Rice. Slip dynamics at an interface between dissimilar materials. *J. Mech. Phys. Solids*, 49:341–361, Feb 2001.

- [11] Y. Ben-Zion. Dynamic ruptures in recent models of earthquake faults. *J. Mech. Phys. Solids*, 49:2209–2244, Sep 2001.
- [12] K. W. Xia, A. J. Rosakis, H. Kanamori, and J. R. Rice. Laboratory earthquakes along inhomogeneous faults: Directionality and supershear. *Science*, 308:681–684, Apr 2005.
- [13] Z. Q. Shi and Y. Ben-Zion. Dynamic rupture on a bimaterial interface governed by slip-weakening friction. *Geophys. J. Int.*, 165:469–484, May 2006.
- [14] A. M. Rubin and J. P. Ampuero. Aftershock asymmetry on a bimaterial interface. *J. Geophys. Res.*, 112, B05307, 2007.
- [15] A. J. Rosakis, K. W. Xia, G. Lykotrafitis, and H. Kanamori. Dynamic shear rupture in frictional interfaces: Speeds, Directionality and Modes. *Treatise in Geophysics*, pages ed. H. Kanamori, vol. 4, 153–192, 2007.
- [16] J. B. Walsh. The Effect of Cracks on the Compressibility of Rocks. *J. Geophys. Res.*, 70(381–389), 1965.
- [17] R. J. O’Connell and B. Budiansky. Seismic velocities in dry and saturated cracked solids. *J. Geophys. Res.*, 79(35):5412–5426, 1974.
- [18] M. Kachanov. Elastic solids with many cracks- A simple method of analysis. *Int. J. Solids. Struct.*, 23(1):23–43, 1987.
- [19] M. Kachanov. On the effective moduli of solids with cavities and cracks. *Int. J. Fract.*, 59(1):17–21, 1993.
- [20] C. M. Sayers and M. Kachanov. Microcrack-induced elastic wave anisotropy of brittle rocks. *J. Geophys. Res.*, 100:4149–4149, 1995.
- [21] V. Lyakhovskiy, Z. Reches, R. Weinberger, and T. E. Scott. Non-linear elastic behaviour of damaged rocks. *Geophys. J. Int.*, 130(1):157–166, 1997.
- [22] B. Budiansky and R. J. O’Connell. Elastic moduli of a cracked solid. *Int. J. Solids. Struct.*, 12(1):81–97, 1976.
- [23] V. Lyakhovskiy, Y. Ben-Zion, and A. Agnon. Distributed damage, faulting, and friction. *J. Geophys. Res.*, 102(27):635–727, 1997.
- [24] V. S. Deshpande and A. G. Evans. Inelastic deformation and energy dissipation in ceramics: A mechanism-based constitutive model. *J. Mech. Phys. Solids*, 56(10):3077–3100, 2008.
- [25] M. F. Ashby and C. G. Sammis. The damage mechanics of brittle solids in compression. *Pure Appl. Geophys.*, 133(3):489–521, 1990.
- [26] J. R. Rice, C. G. Sammis, and R. Parsons. Off-fault secondary failure induced by a dynamic slip pulse. *Bull. Seismol. Soc. Amer.*, 95(1):109–134, 2005.